Zoosyst. Evol. 101 (4) 2025, 2103–2121 | DOI 10.3897/zse.101.163559

PENSOFT

für Naturkunde MUSEUM FÜR NATURKUNDE BERLIN

Morphology and phylogeny of two new species of deep-sea mushroom soft corals (Octocorallia, Corallidae, Anthomastinae) from the Southern Mid-Atlantic Ridge

Xinlong Li[1,2], Ningxia Xu[1,2], Meiling Ge[1,2], Xuying Hu[1,2], Mengna Li[3], Zongling Wang[1,2], Xuelei Zhang[1,2], Qinzeng Xu[1,2]

1 *Key Laboratory of Marine Eco-Environmental Science and Technology, First Institute of Oceanography, MNR, Qingdao 266061, China*

2 *Laboratory for Marine Ecology and Environmental Science, Qingdao Marine Science and Technology Center, Qingdao 266100, China*

3 *National Deep Sea Center, MNR, Qingdao 266237, China*

https://zoobank.org/BBB6DED7-18E3-4706-A9EA-D31797EA00EF

Corresponding author: Qinzeng Xu (xqz08@163.com)

Academic editor: Pavel Stoev ♦ **Received** 29 June 2025 ♦ **Accepted** 19 October 2025 ♦ **Published** 5 November 2025

Abstract

Members of the subfamily Anthomastinae Verrill, 1922, commonly known as mushroom soft corals, are characterized by their capitate or mushroom-shaped red colonies and large autozooids. Deep-sea mushroom corals of this subfamily remain poorly documented in the South Atlantic. This study describes two new Anthomastinae species, *Neoanthomastus longistylus* **sp. nov.** and *Anthomastus mirabilis* **sp. nov.**, from the Southern Mid-Atlantic Ridge at depths of 1,553–2,145 m. *Neoanthomastus longistylus* **sp. nov.** is characterized by a slender stalk, siphonozooids distributed on the capitulum and the upper third of the stalk, and tentacular sclerites that are predominantly straight rods and rods with one end curved. *Anthomastus mirabilis* **sp. nov.** is distinguished by the presence of dumbbells in its tentacles, clubs and dumbbells in the anthocodial wall, and the absence of spindles. The mitochondrial genome of *N. longistylus* **sp. nov.** contains 14 PCGs, 2 rRNAs, and 1 tRNA, while that of *A. mirabilis* **sp. nov.** comprises 17 PCGs, 2 rRNAs, and 1 tRNA, with three duplicated genes – ND3, ND6, and ND4L – that are identical in sequence. Phylogenetic analyses based on the partial *mtMutS* gene and 13 PCGs from the mitochondrial genomes (*mtMutS* not included) reveal the phylogenetic relationships within the subfamily Anthomastinae. These are the first records of both genera from the Southern Mid-Atlantic Ridge, enriching the known species diversity and providing critical baseline data for future biodiversity assessments.

Key Words

Anthomastus, mitochondrial genome, *Neoanthomastus*, phylogenetic analysis, Southern Mid-Atlantic Ridge

Introduction

The family Coralliidae Lamouroux, 1812 exhibits remarkable morphological diversity, with species displaying diverse axial structures – from absent axes to those composed of unfused sclerites, and finally to fully fused scleritic axes (Bayer 1993; Debreuil et al. 2011; McFadden et al. 2022). Within this family, the subfamily Anthomastinae is distinguished by its lack of an axial skeleton. Unlike Coralliidae and Paragorgiidae, in which autozooids occur along the axial branches, most Anthomastinae have the autozooid anthocodia concentrated over the capitulum; in a few species, siphonozooids also occur on the stalk. (Molodtsova 2013; Li et al. 2025). Their mushroom-like appearance makes them easily distinguishable from other coral groups.

The classification of Anthomastinae has undergone significant revision in recent years. Anthomastinae was historically placed within the family Alcyoniidae due to morphological similarities with genera such as *Alcyonium* Linnaeus, 1758, *Bellonella* Gray, 1862, and *Eleutherobia* Pütter, 1900 (Thomson 1911, Verseveldt and Bayer 1988; Williams 2003). Berntson et al. (2001)

Copyright *Li, X. et al.* This is an open access article distributed under the terms of the Creative Commons Attribution License (CC BY 4.0), which permits unrestricted use, distribution, and reproduction in any medium, provided the original author and source are credited.

revealed that *Anthomastus* is genetically closer to *Corallium* based on nuclear *18S rRNA*. Anthomastinae was transferred to Coralliidae based on an ultra-conserved elements/exon phylogenomic analysis by McFadden et al. (2022), which reconstructed maximum likelihood trees from 739 loci (60% taxon occupancy). Li et al. (2025) reconstructed the phylogenetic relationships for the five genera within the subfamily Anthomastinae, which are *Anthomastus* Verrill, 1878; *Bathyalcyon* Versluys, 1906; *Heteropolypus* Tixier-Durivault, 1964; *Pseudoanthomastus* Tixier-Durivault & d'Hondt, 1974; and *Neoanthomastus* Li, Li & Xu, 2025, a genus newly established by the authors.

The subfamily Anthomastinae is widely distributed across the North Atlantic, Indian, Pacific, and the Southern Ocean, with a predominant presence in deep-sea environments (>200 m depth; Molodtsova 2013; Li and Xu 2023). The first described species, *Anthomastus grandiflorus* Verrill, 1878, was reported from the North Atlantic (Verrill 1879). Subsequently, Anthomastinae species, especially *Anthomastus*, *Pseudoanthomastus*, and *Neoanthomastus*, have been documented across the North Atlantic, including coastal waters near continental margins and islands, as well as along the Northern Mid-Atlantic Ridge. The South Atlantic features complex topography, including the Southern Mid-Atlantic Ridge (SMAR), and a rich coral fauna. Shallow-water reefs (e.g., Brazil's Abrolhos Bank) and deep-sea corals (e.g., *Desmophyllum pertusum*) are well-documented in this region (Leão and Kikuchi 2001; Carvalho et al. 2023). Data from OBIS and GBIF reveal occurrences of Anthomastinae in the coastal South Atlantic and near its southern islands. However, the deep seamounts of the SMAR lack any confirmed records of Anthomastinae. Recent discoveries of new coral species at the Carlsberg Ridge (Hu et al. 2025) further suggest that deep-sea ecosystems may harbor numerous undescribed taxa, highlighting the need for targeted exploration.

During a benthic fauna survey of the South Atlantic Mid-Ocean Ridge, we collected samples of Anthomastinae and discovered two new species. By combining morphological taxonomic identification with molecular phylogenetic analysis, this study aims to enhance our understanding of deep-sea coral species in the Southern Mid-Atlantic Ridge.

Materials and methods

Specimen collection and morphological analyses

Eight specimens were collected in 2024 using the *Jiaolong* Human-Operated Vehicle (HOV) during China's Ocean 83 Cruise organized by the National Deep Sea Center (NDSC) aboard the R/V *Shenhai Yihao* from the Southern Mid-Atlantic Ridge (Table 1). These specimens were photographed *in situ* before being sampled and photographed again on board. The collected samples were preserved using three methods: alcohol preservation, RNAlater Stabilization Solution, and rapid freezing in liquid nitrogen. All type materials have been permanently deposited in the Key Laboratory of Marine Eco-Environmental Science and Technology, First Institute of Oceanography located in Qingdao, China. The voucher numbers for these specimens are provided in Table 1.

The shape and color of the capitulum and stalk were observed, the number of autozooids was counted, and their size was measured. Using a Nikon SMZ1270 stereomicroscope, we examined and photographed the external surfaces of the capitulum and autozooid tentacles. We then dissected the capitulum and stalk to inspect the interior tissues. The specimens were dissected using dissecting needles and scalpels into six parts: autozooid tentacles, pharynx, anthocodial wall, capitulum surface, stalk, and holdfast. These parts were separately soaked in a 10% sodium hypochlorite solution for 1–2 hours until the soft tissues were completely dissolved. The resulting sclerites were cleaned with distilled water and anhydrous ethanol, then placed on double-sided insulating tape. After drying, the samples were gold-sprayed and observed under a Regulus8100 scanning electron microscope. The sclerites were classified according to standard taxonomic conventions (Bayer 1956; Bayer et al. 1983).

DNA extraction and sequencing

Polyps were collected into 1.5 mL sterile centrifuge tubes. Total genomic DNA was extracted using the MicroElute Genomic DNA Kit (OMEGA, USA). DNA concentration and purity were measured using a spectrophotometer. Ac-

Table 1. Geographical data for eight mushroom soft coral specimens collected from the Southern Mid-Atlantic Ridge.

Voucher number	Latitude, Longitude	Depth (m)	Species
FIO-ATL83-JLBEN26602	22°58'45"S, 13°32'34"W	1929	*Neoanthomastus longistylus* sp. nov.
FIO-ATL83-JLBEN26603	22°58'44"S, 13°32'35"W	1928	*Neoanthomastus longistylus* sp. nov.
FIO-ATL83-JLBEN26604	22°59'2"S, 13°32'14"W	1860	*Neoanthomastus longistylus* sp. nov.
FIO-ATL83-JLBEN26704	22°59'3"S, 13°29'31"W	2151	*Neoanthomastus longistylus* sp. nov.
FIO-ATL83-JLBEN26705	22°58'56"S, 13°29'50"W	2145	*Neoanthomastus longistylus* sp. nov.
FIO-ATL83-JLBEN27711	14°3'28"S, 14°20'53"W	1649	*Anthomastus mirabilis* sp. nov.
FIO-ATL83-JLBEN27712	14°3'31"S, 14°20'50"W	1649	*Anthomastus mirabilis* sp. nov.
FIO-ATL83-JLBEN27713	14°3'30"S, 14°20'48"W	1649	*Anthomastus mirabilis* sp. nov.

ceptable criteria included an A260/A280 ratio between 1.8 and 2.0, an A260/A230 ratio greater than 1.8, and a concentration above 100 ng/μL. The extracted DNA was sequenced on the Illumina platform by Novogene Technology, Inc. (Beijing, China). Additionally, the *mtMutS* gene was amplified using primers AnthoCorMSH (5'-AGGAGAATTATTCTAAGTATGG-3'; Herrera et al., 2010) and Mut-3458R (5'-TSGAGCAAAAGCCACTCC-3'; Sánchez et al., 2003). The PCR reaction mixture (25 μL) contained: 1 μL of template DNA, 1 μL of each primer (0.4 μM), 12.5 μL of 2× Taq Plus Master Mix, and 9.5 μL of ddH_2O. The PCR amplification protocol included an initial denaturation at 98 °C for 2 minutes, followed by 32 cycles (denaturation at 98 °C for 15 seconds, annealing at 50 °C for 15 seconds, extension at 72 °C for 60 seconds), with a final extension at 72 °C for 2 minutes. Each sample was amplified in triplicate. PCR products were visualized using 2% agarose gel electrophoresis and sequenced bidirectionally using Sanger sequencing at Sangon Biotech, Inc. (Qingdao, China), with the same primers.

Mitogenome data assembly and annotation

The mitochondrial genome was assembled using GetOrganelle v1.7.5 (Jin et al. 2020). Gene annotation, including protein-coding genes (PCGs), tRNAs, and rRNAs, was conducted using MITOS2 (https://usegalaxy.eu). To enhance the precision of tRNA gene identification, tRNAscan-SE (https://trna.ucsc.edu/tRNAscan-SE/) was employed. PCGs were translated into amino acid sequences based on the mold, protozoan, and coelenterate mitochondrial genetic code (translation table 4). Initial gene predictions generated by MITOS were further refined by removing redundant annotations and manually adjusting start and stop codon positions. Finally, the complete circular mitogenome was visualized using Proksee (https://proksee.ca/). To verify the presence of duplicated genes in the mitochondrial genome of *Anthomastus mirabilis* sp. nov., primers were designed using Primer5, and PCR amplification and sequencing were performed following the same protocol described above (Suppl. material 1: table S1). All sequence data generated in this study have been deposited in the NCBI database (Suppl. material 1: table S3).

Phylogenetic analyses

A total of 47 partial *mtMutS* sequences were analyzed, including 8 from this study (*N. longistylus* sp. nov. and *A. mirabilis* sp. nov.), 35 from the NCBI database for the subfamily Anthomastinae, and 4 sequences from genera outside of Anthomastinae within Coralliidae (outgroups). PhyloSuite was utilized to conduct phylogenetic analyses using both Maximum Likelihood and Bayesian methods. All sequences were aligned in batches with MAFFT v7.505 (Katoh and Standley 2013), and then trimmed with Gblocks v0.91. ModelFinder v2.2.0 (Kalyaanamoorthy et al. 2017) was used to select the best-fit model. Maximum likelihood phylogenies were inferred using IQ-TREE v2.2.0 (Nguyen et al. 2015) under the HKY+F model for 5000 ultrafast bootstraps. Bayesian inference (BI) phylogenies were reconstructed using MrBayes v3.2.7a (Ronquist et al. 2012) under HKY+F model. Four independent runs were conducted, each consisting of four Markov Chain Monte Carlo (MCMC) chains, run for 2 million generations. The first 25% of sampled trees from each run were discarded as burn-in to ensure convergence. A total of 35 complete mitochondrial genome sequences were analyzed, including 6 from this study, 23 from the NCBI database for the subfamily Anthomastinae, and 6 sequences from genera outside of Anthomastinae within Coralliidae (outgroups). Thirteen protein-coding genes (PCGs) were extracted using PhyloSuite v1.2.3 (Zhang et al. 2020; Xiang et al. 2023), then aligned in batches and trimmed using MAFFT v7.505 and Gblocks v0.91. Substitution models were selected for each gene using ModelFinder v2.2.0 (Kalyaanamoorthy et al. 2017) under the Bayesian Information Criterion (BIC). An edge-linked partition scheme was employed, and the selected models were subsequently used for phylogenetic inference. The remaining steps for tree construction followed the same approach as those used for the partial *mtMutS* dataset. The best-fit models and partitioning schemes for BI and ML are shown in Suppl. material 1: table S2. The phylogenetic tree was visualized using the Interactive Tree of Life (iTOL) website (https://itol.embl.de/). To assess the genetic divergence among and within different species, we calculated genetic distances with Mega 7, employing the Kimura 2-Parameter model on the concatenated 14 PCGs of mitochondrial genomes.

Results

Morphological taxonomy

Class Octocorallia Haeckel, 1866
Order Scleralcyonacea McFadden, van Ofwegen & Quattrini, 2022
Family Coralliidae Lamouroux, 1812
Subfamily Anthomastinae Verrill, 1922

Genus *Neoanthomastus* Li, Li & Xu, 2025

Neoanthomastus Li, Li & Xu, 2025: 12.

Diagnosis. (Modified from Li et al. 2025, with bold italics indicating modifications.) Mushroom-shaped, capitate colonies with dome-shaped capitulum separated from a conspicuous and often cylindrical stalk. Polyps dimorphic, with sclerites. Autozooids arranged over capitulum, sterile, large, not very numerous, retractile but not completely retracted. Sclerites equally developed around

autozooids. Anthocodial armature more developed near base of tentacles. Siphonozooids scattered over both capitulum and stalk, fertile, conspicuous, feebly armored, and numerous. Sclerites multiradiates, rods, spindles, needles, ***clubs, and crosses***. Pharyngeal sclerites predominantly rodlets, sometimes with *crosses*. Tentacular sclerites predominately rods, spindles, and multiradiates.

Type species. *Neoanthomastus stellatus* Li, Li & Xu, 2025.

Neoanthomastus longistylus Li & Xu, sp. nov.

https://zoobank.org/CF57044D-6FB2-43F5-9E3F-7219BD41ADAD

Figs 2–5

Material examined. ***Holotype*** • FIO-ATL83-JLBEN26604, collected by Qinzeng Xu using the HOV Jiaolong from the R/V *Shenhai Yihao* on 14 February 2024 at station JL266 (22°59'2"S, 13°32'14"W), Southern Mid-Atlantic Ridge, at a depth of 1,860 m.

Paratypes • Two specimens (FIO-ATL83-JLBEN26602, part of a colony; FIO-ATL83-JLBEN26603), same station as for holotype • Two specimens (FIO-ATL83-JLBEN26704; FIO-ATL83-JLBEN26705, part of a colony), collected with the same vessel, gear, and by the same collectors as the holotype, on 15 February 2024 at station JL267 (22°58'56"S, 13°29'50"W), Southern Mid-Atlantic Ridge, at a depth of 2,150 m.

Diagnosis. Mushroom-shaped, capitate colony with a spherical capitulum separated from a cylindrical stalk. Stalk is long, typically at least three times longer than its maximum width, and approximately 2.5 times longer than the capitulum. Autozooids are large, retractile but not completely retracted. Siphonozooids are red, small, visible, and distributed across the surface of the capitulum and restricted to the upper 1/3 of the stalk. Sclerites include rods, clubs, spindles, multiradiates, and crosses; sclerite density on the capitulum surface, tentacles, and pharynx is abundant. Sclerites from the interior of the capitulum are absent. Anthocodial walls contain both curved rods and clubs. Pharyngeal sclerites are rodlets and crosses. Tentacular sclerites consist exclusively of straight rods and rods with one end unilaterally curved, lacking spindles and multiradiates.

Description of holotype. ***Colony form and size.*** The specimen FIO-ATL83-JLBEN26604 is a mushroom-shaped, capitate colony with a spheroidal capitulum supported by a conspicuous stalk (Fig. 1B). The capitulum is 17 mm in diameter and 15 mm high. The transition between the capitulum and the stalk is smooth. The conspicuous, longitudinally striated stalk is long (45 mm in height, 75% of the colony), soft, and gradually tapers toward the capitulum (6 mm in diameter), while the base of the stalk is thicker (14 mm in diameter). In life, the specimen was attached to stone (Fig. 1B).

Polyps. The polyps are dimorphic. 28 autozooids are evenly arranged on the capitulum, retractile but not completely retracted. Upon retraction, the tentacles first contract into a spherical shape, followed by the autozooids retracting into the capitulum, leaving a protrusion on the surface of the capitulum. The largest autozooid has a diameter of 5 mm and a length of 33 mm, including the tentacles. The tentacles reach up to 12 mm with mostly 14–18 pairs of pinnules. The longest pinnules are located at the distal third of the tentacles. Siphonozooids are distributed on the capitulum and the upper third of the stalk, visible as red protrusions, and are usually 0.4–0.6 mm wide, spaced 0.15–0.6 mm apart (Fig. 1D).

Sclerites. Tentacular sclerites (Fig. 2A) are exclusively composed of rods, including straight rods (0.17–0.35 mm long) and rods with one end curved (0.18–0.34 mm long). Pharyngeal sclerites (Fig. 2B) are mostly rodlets (0.06–0.09 mm long) and a few crosses. Anthocodial sclerites (Fig. 3A) are straight rods (0.16–0.36 mm long), rods with one end curved (0.16–0.37 mm long), and a few clubs (0.18–0.25 mm long). Sclerites from the surface of capitulum (Fig. 3B) are straight rods (0.31–0.35 mm long), rods with one end curved (0.23–0.30 mm long), prominent tuberculated spindles (0.17–0.24 mm long), prominent tuberculated clubs (0.18–0.23 mm long), and multiradiates (0.12–0.15 mm long). Sclerites from surface of the stalk (Fig. 4A) are mostly multiradiates (0.11–0.14 mm long), a few rods (0.31–0.34 mm long), and prominent tuberculated spindles (0.15–0.28 mm long). Sclerites from interior of the stalk (Fig. 4B) are mostly rods (0.15–0.23 mm long) and a few rods with a short transverse axis (0.18–0.20 mm long). Sclerites of the holdfast (Fig. 4C) are rods (0.23–0.31 mm long), multiradiates (0.12–0.15 mm long), prominent tuberculated spindles (0.15–0.25 mm long), a few rods with a short transverse axis (0.22–0.27 mm long), and crosses. Sclerites from the interior of the capitulum are absent.

Color. In alcohol, both the capitulum and the stalk appear red, with the stalk being slightly lighter in color than the capitulum. The tentacle tips and pinnules are pale yellow, and the sclerites are red.

Variation. Paratype FIO-ATL83-JLBEN26602 is large, measuring 120 mm in total height, with a stalk height of 95 mm and bearing 28 autozooids. Paratype FIO-ATL83-JLBEN26603 is attached to a dead coral branch, with a total height of 50 mm. The stalk measures 35 mm, approximately twice the height of the capitulum, and bears 12 autozooids. FIO-ATL83-JLBEN26704 measures 75 mm in total height, with a stalk height of 55 mm and bears 18 autozooids. FIO-ATL83-JLBEN26705 has a total height of 90 mm, with a stalk height of 72 mm and a relatively small capitulum (18 mm) bearing 9 autozooids.

Etymology. The specific name *longistylus* refers to the long stalk, one of the characteristics of this species.

Distribution and habitat. Known only from the Southern Mid-Atlantic Ridge, 1,860–2,151 m.

Remarks. *N. longistylus* sp. nov. has siphonozooids distributed across the capitulum's surface and extending onto the stalk, with pharyngeal sclerites that are mostly rodlets. These characteristics distinguish it from other genera in the subfamily, placing it within the genus *Neoanthomastus*.

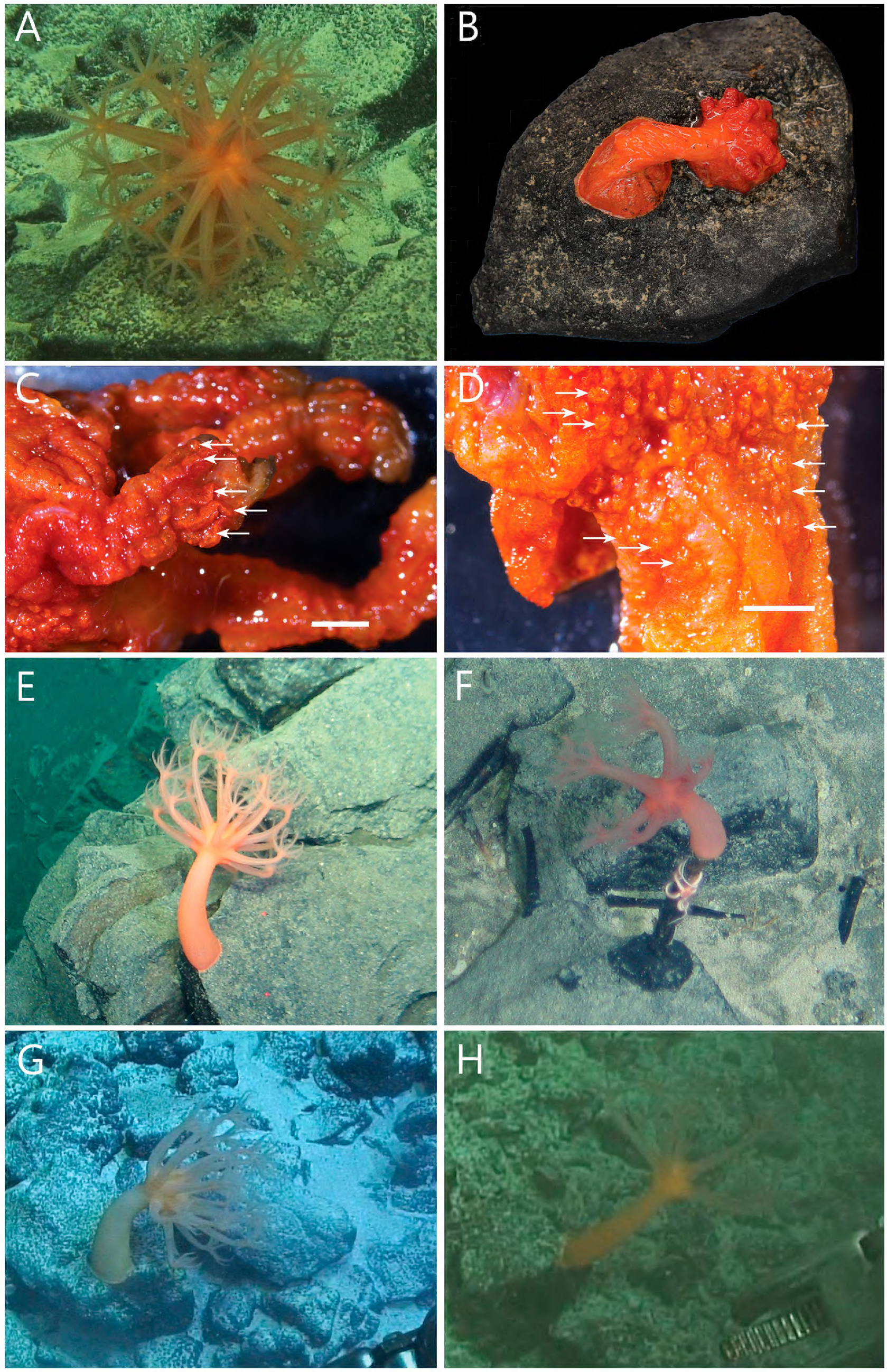

Figure 1. Morphology of *Neoanthomastus longistylus* sp. nov. **A–D**. The holotype FIO-ATL83-JLBEN26604: **A.** In situ view; **B.** Colony; **C.** The tentacles of autozooids, indicated by arrows; **D.** The siphonozooids, indicated by arrows. **E–H.** Paratypes showing colony morphology: **E.** FIO-ATL83-JLBEN26602; **F.** FIO-ATL83-JLBEN26603; **G.** FIO-ATL83-JLBEN26704; **H.** FIO-ATL83-JLBEN26705. Scale bars: 10 mm (**B**); 2 mm (**C, E**).

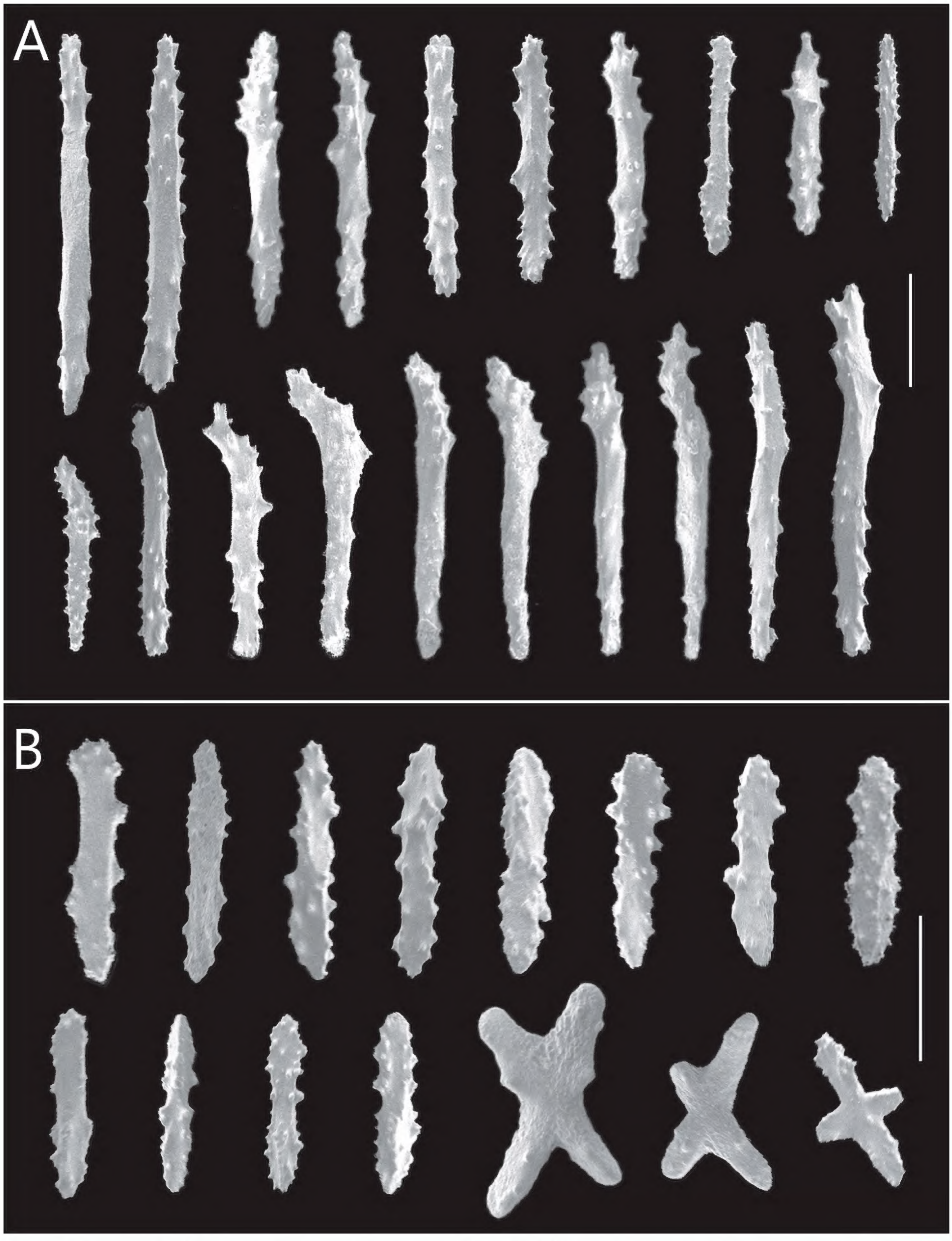

Figure 2. Sclerites of *Neoanthomastus longistylus* sp. nov. (FIO-ATL83-JLBEN26604). **A.** Sclerites from autozooid tentacles; **B.** Sclerites from pharynx. Scale bars: 0.10 mm (**A**); 0.05 mm (**B**).

N. longistylus sp. nov. resembles *N. giganteus* in having an elongated stalk, siphonozooids scattered on the upper 1/3 of stalk. However, their sclerite characteristics differ. *N. longistylus* sp. nov. has abundant sclerites on its tentacles, pharynx, and capitulum surface, in contrast to *N. giganteus* (Tixier-Durivault, 1954), which has sparse sclerites.

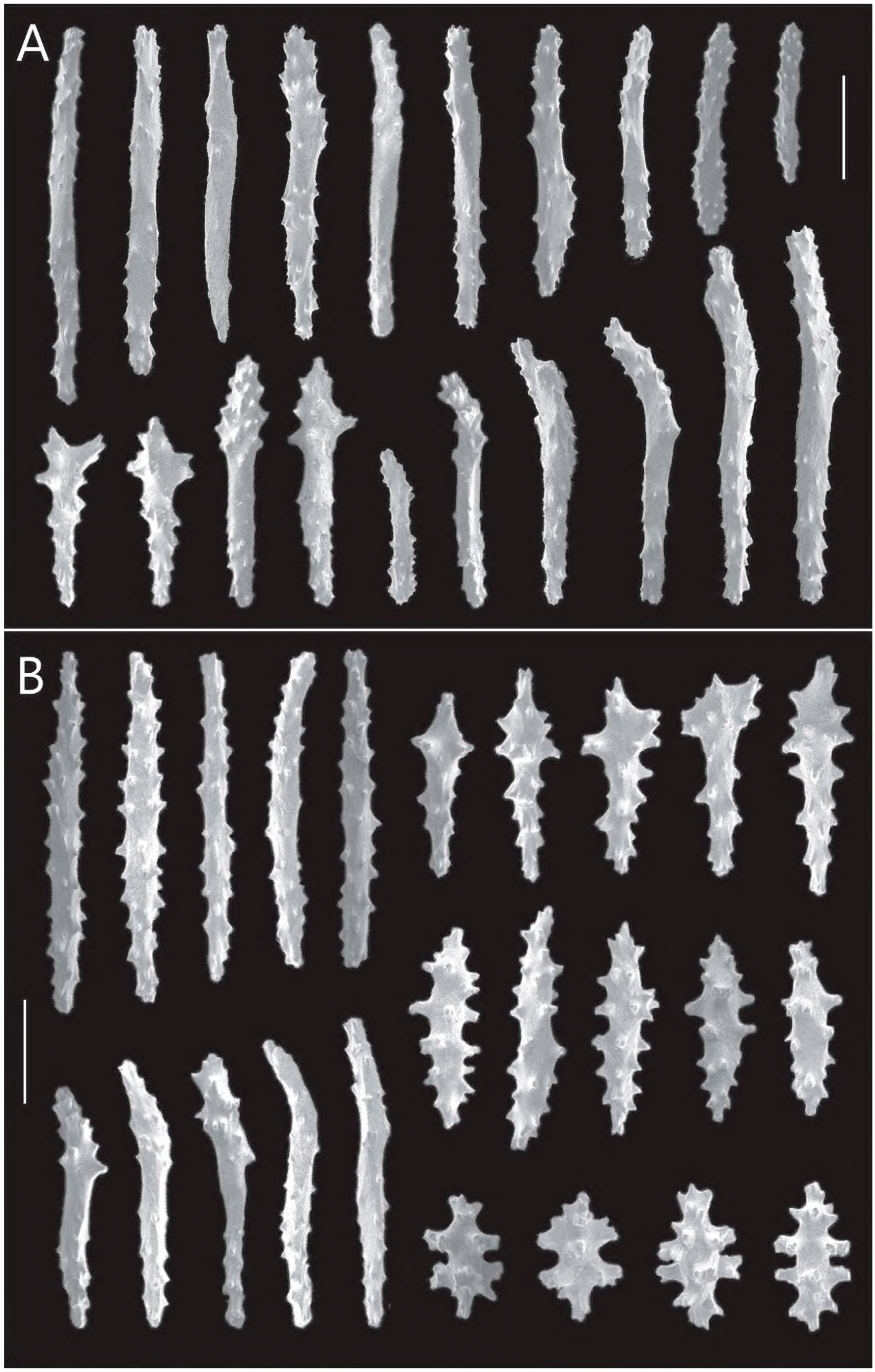

Figure 3. Sclerites of *Neoanthomastus longistylus* sp. nov. (FIO-ATL83-JLBEN26604). **A.** Sclerites from anthocodial wall; **B.** Sclerites from surface of capitulum. Scale bars: 0.10 mm.

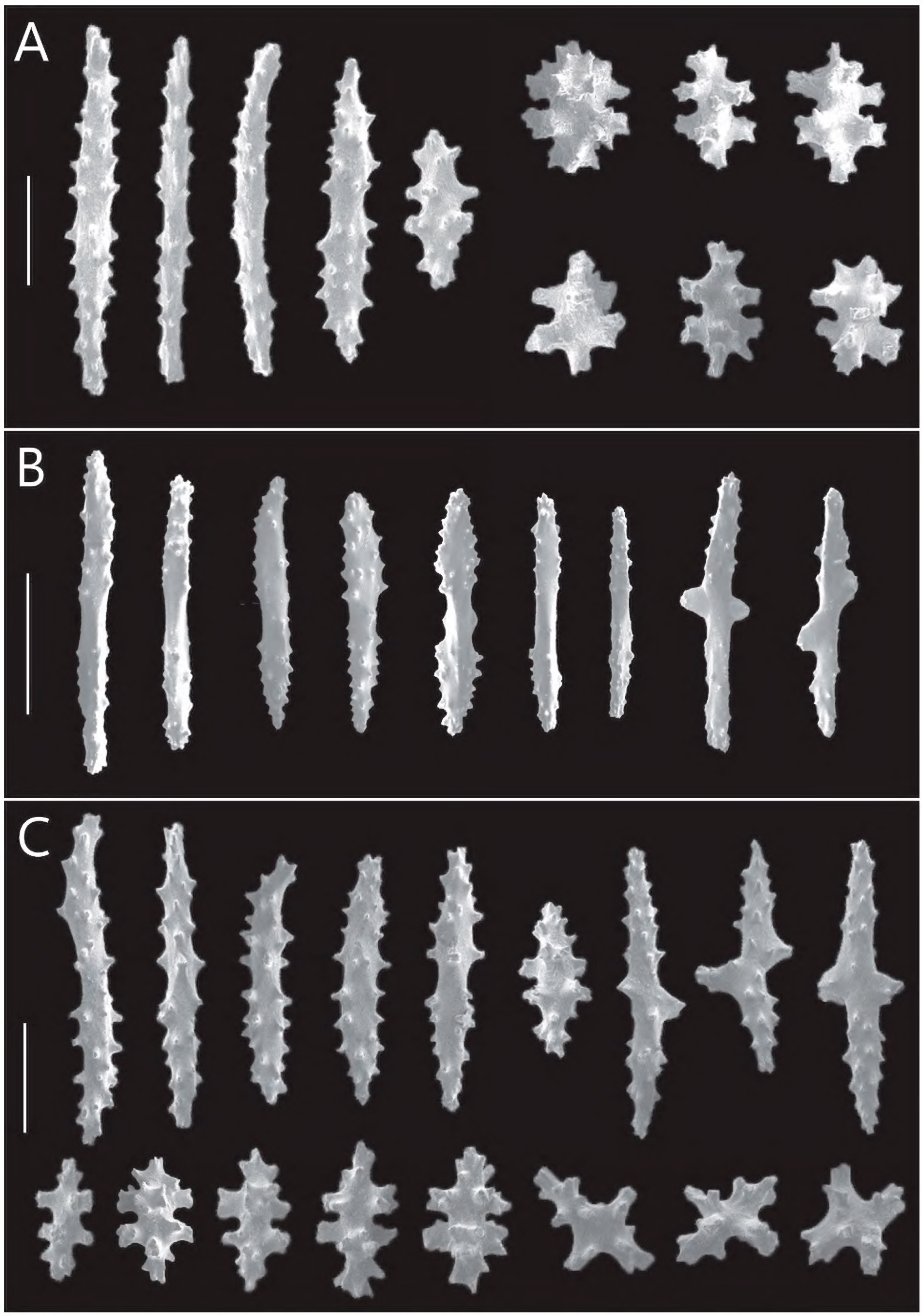

Figure 4. Sclerites of *Neoanthomastus longistylus* sp. nov. (FIO-ATL83-JLBEN26604). **A.** Sclerites from surface of stalk; **B.** Sclerites from interior of stalk; **C.** Sclerites from holdfast. Scale bars: 0.10 mm.

The autozooid tentacles of *N. longistylus* sp. nov. contain unilaterally curved rods, and its anthocodial walls have both curved rods and clubs, features absent in *N. giganteus*. The surface of *N. longistylus* sp. nov. lacks the spiny dumbbells found on N. giganteus. In addition, *N. longistylus* sp. nov. colonies are soft and mostly curved, while *N. giganteus* colonies are rigid.

Beyond *N. giganteus*, the new species is also clearly separated from all other members of the genus. It is distinguished from *N. purpureus* and *N. hicksoni* by possessing a distinctly elongated stalk (at least three times longer than wide), as opposed to their short stalks. Furthermore, *N. longistylus* sp. nov. differs from *N. stellatus*, *N. tahinodus*, and *N. elongatus*, which have siphonozooids covering the entire stalk, whereas the siphonozooids of the new species are restricted to the upper one-third.

Anthomastus Verrill, 1878

Anthomastus mirabilis Li & Xu, sp. nov.

https://zoobank.org/71F758BF-6C8E-4F9E-B9C6-EABAD67A781C

Figs 5–8

Material examined. ***Holotype*** • FIO-ATL83-JLBEN27711, collected by Qinzeng Xu using the HOV Jiaolong from the R/V *Shenhai Yihao* on 28 February 2024 at station JL277 (14°3'28"S, 14°20'53"W), Southern Mid-Atlantic Ridge, at a depth of 1,553 m.

Paratypes • FIO-ATL83-JLBEN27712 and FIO-ATL83-JLBEN27713 were collected together with holotype.

Diagnosis. Mushroom-shaped, with a spherical capitulum and a short and inconspicuous stalk. Polyps are dimorphic. Autozooids are large, retractile, and evenly arranged over the capitulum. Siphonozooids are invisible, numerous, densely scattered among autozooids. The sclerite profile is diverse, but characterized by the absence of spindles in all parts of the colony. Sclerites of the capitulum surface and stalk predominantly include multiradiates and plates. Tentacular sclerites are composed predominantly of dumbbells and plates; anthocodial walls contain clubs and dumbbells. Pharyngeal sclerites are platelets with a distinct median waist and crosses.

Description of holotype. ***Colony form and size.*** The specimen FIO-ATL83-JLBEN27711 has a prominent capitulum supported by an inconspicuous stalk, with an approximate 1:1 height ratio between the capitulum and stalk, and a total height of 42 mm (Fig. 6A, G). The capitulum is dome-shaped, with a diameter of 33 mm and a height of 20 mm. The stalk is short, thick, and cylindrical, with a diameter of 20 mm and a height of 22 mm.

Polyps. There are 22 large autozooids evenly arranged over the capitulum, typically spaced about 8 mm apart. The autozooids are retractile, with some being fully retracted while others are contracted with their tentacles curved inward, forming small spherical protrusions on the surface of capitulum (Fig. 5C). The autozooids are large, with a maximum length of 51 mm (including tentacles, which are 17 mm long). The pinnules are arranged either oppositely or alternately, with 12–18 pairs. Siphonozooids are small, numerous, invisible, and scattered among the autozooids at intervals of 1.6–2.0 mm.

Sclerites. Tentacular sclerites (Fig. 6A) are plates (0.12–0.21 mm long), rods (0.13–0.23 mm long), dumbbells (0.11–0.22 mm long), and a few rods with a short transverse axis (0.14–0.23 mm long). Pharyngeal sclerites (Fig. 6B) are platelets with a median waist (0.05–0.08 mm long) and a few crosses derived from small plates. Sclerites of the anthocodial wall (Fig. 7A) are rods (0.17–0.35 mm long), clubs (0.14–0.19 mm long), dumbbells (0.13–0.18 mm long), multiradiates (0.10–0.14 mm long), and a few crosses. Sclerites from the surface of capitulum (Fig. 7B) are rods (0.18–0.37 mm long), clubs (0.17–0.23 mm long), multiradiates (0.11–0.14 mm long), and a few crosses. Sclerites from interior of capitulum (Fig. 7C) are long rods (0.27–0.49 mm long). Sclerites from the surface of stalk (Fig. 8A) are multiradiates (0.10–0.14 mm long), rods (0.15–0.23 mm long), and a few crosses. Sclerites from the interior of the stalk (Fig. 8B) are long rods (0.32–0.40 mm long). Sclerites of the holdfast (Fig. 8C) are rods (0.17–0.31 mm long), multiradiates (0.09–0.14 mm long), and a few crosses.

Color. Live specimens display a bright red color, while appearing vermilion in ethanol. The distal ends of the tentacles are yellowish-white.

Variation. Paratype FIO-ATL83-JLBEN27712 was attached to a dead coral skeleton and has 20 autozooids. The capitulum is 16 mm high with a diameter of 23 mm. The stalk is short and inconspicuous, with a length of 6 mm. Paratype FIO-ATL83-JLBEN27713 was also attached to a dead coral skeleton and has 28 autozooids. The capitulum is 22 mm high with a diameter of 33 mm, and the stalk is 16 mm high.

Etymology. The Latin *mirabilis*, meaning "wonderful" and "astonishing," concisely reflects how this deep-sea coral's striking red, spherical form with long autozooids captivates observers with its beauty.

Distribution and habitat. Known only from the type locality. Southern Mid-Atlantic Ridge, 1,553–1,649 m.

Remarks. The morphological characteristics of *Anthomastus mirabilis* sp. nov. match well with the generic definition of *Anthomastus*. Morphologically, *A. mirabilis* sp. nov. is most closely allied with *A. grandiflorus* Verrill, 1878, showing no obvious differences in the external morphology of the capitulum, stalk, and polyps. Both species are grouped by having platelets as the predominant pharyngeal sclerites and by having autozooids distributed across the whole capitulum. However, they are fundamentally separated by their sclerite composition: *A. mirabilis* sp. nov. possesses dumbbells and more plates in its tentacles, and clubs and dumbbells in its anthocodial wall. Crucially, *A. mirabilis* sp. nov. lacks spindles throughout the colony (capitulum, stalk, and holdfast), which is a key distinction from *A. grandiflorus*, for which spindles are a central diagnostic feature.

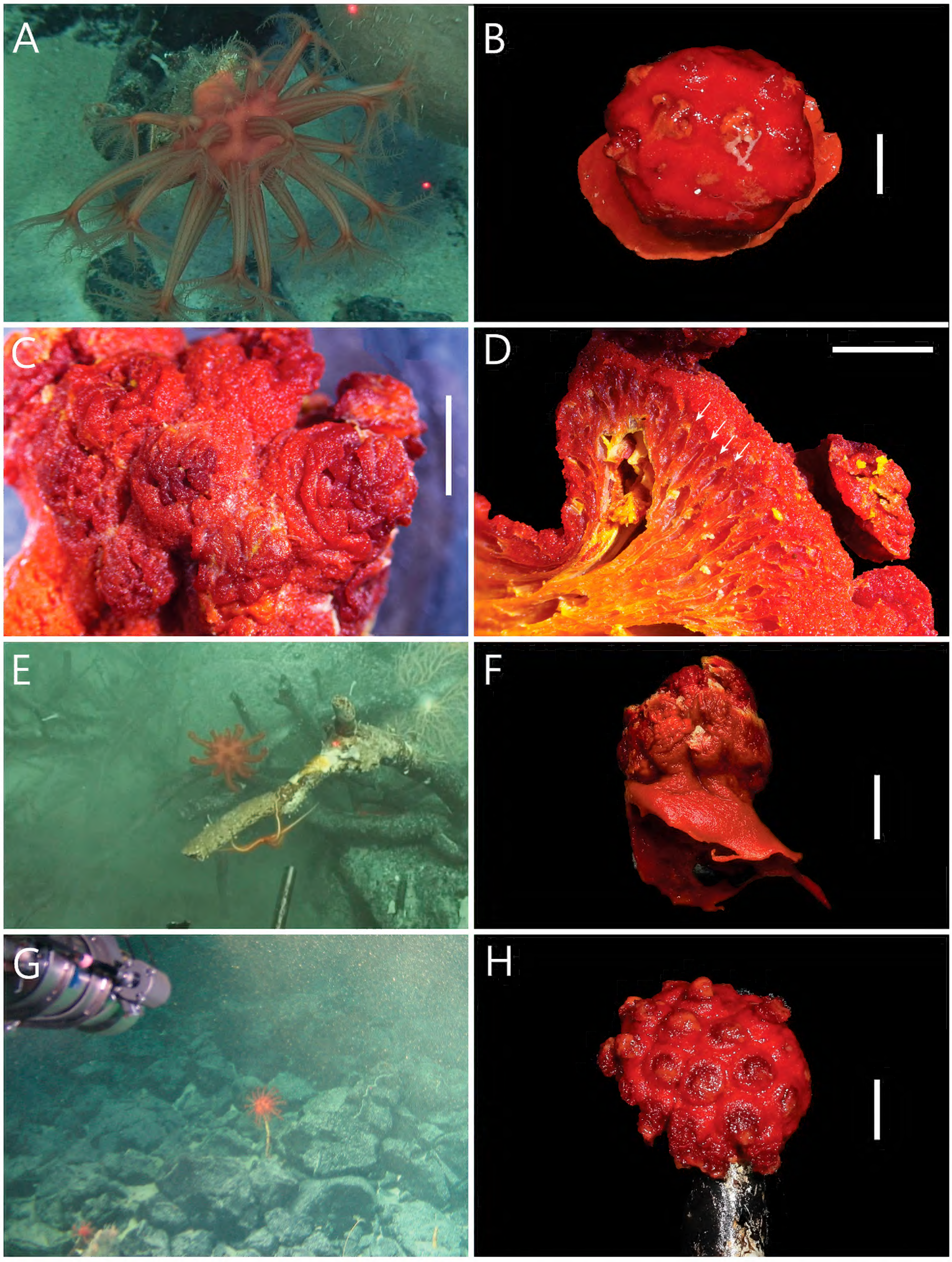

Figure 5. Morphological observation of *Anthomastus mirabilis* sp. nov. **A–D.** The holotype FIO-ATL83-JLBEN27711: **A.** In situ view; **B.** Colony; **C.** Autozooids; **D.** the longitudinal section of capitulum, showing siphonozooids (arrows). **E–H.** Paratypes: FIO-ATL83-JLBEN27712 in situ (**E**) and in preservation (**F**); FIO-ATL83-JLBEN27713 in situ (**G**) and in preservation (**H**). Scale bars: 10 mm (**B, D, F, H**); 5 mm (**C**).

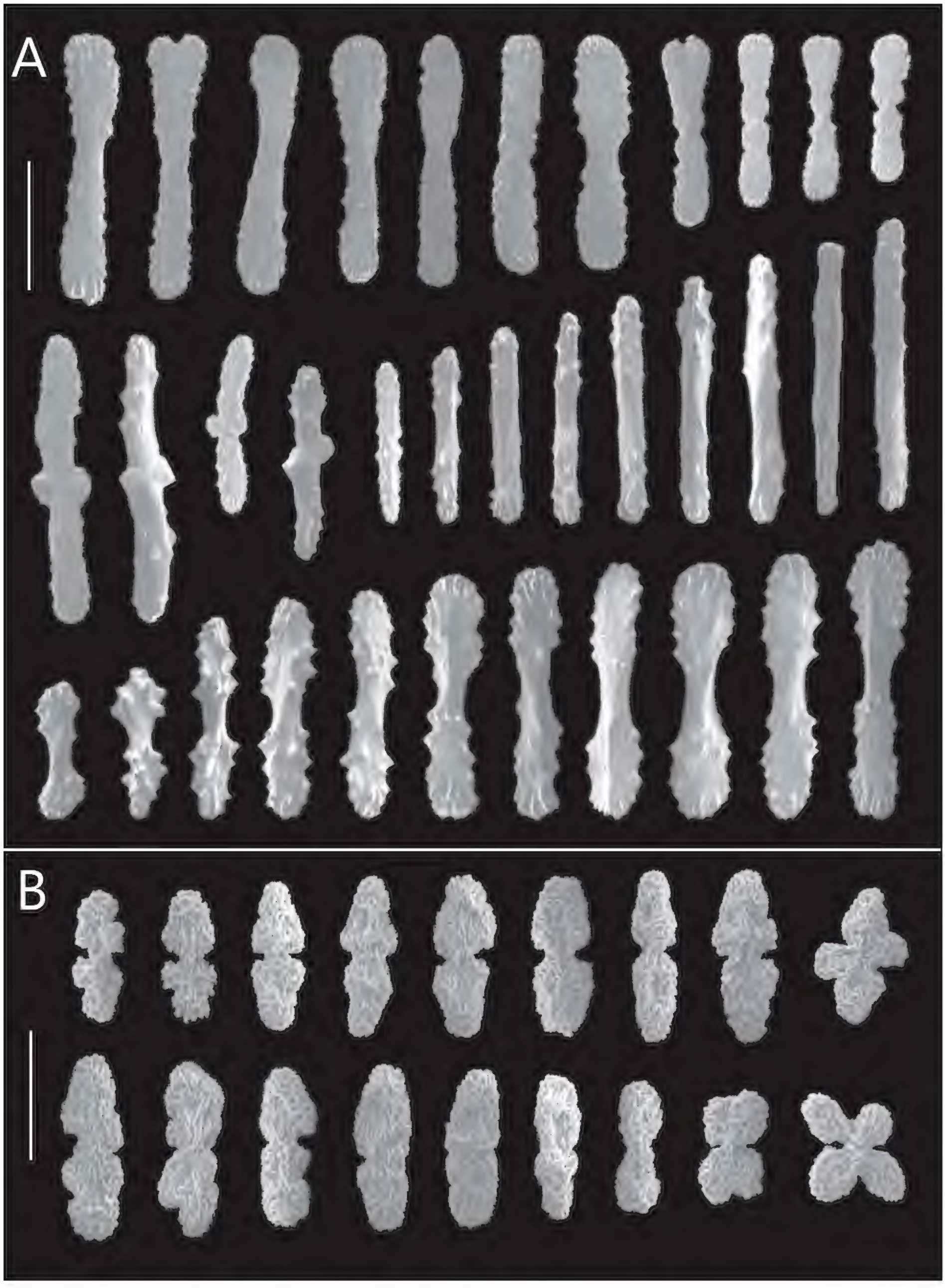

Figure 6. Sclerites of *Anthomastus mirabilis* sp. nov. (FIO-ATL83-JLBEN27711). **A.** Sclerites from autozooid tentacles; **B.** Sclerites from pharynx, Scale bars: 0.10 mm (**A**); 0.05 mm (**B**).

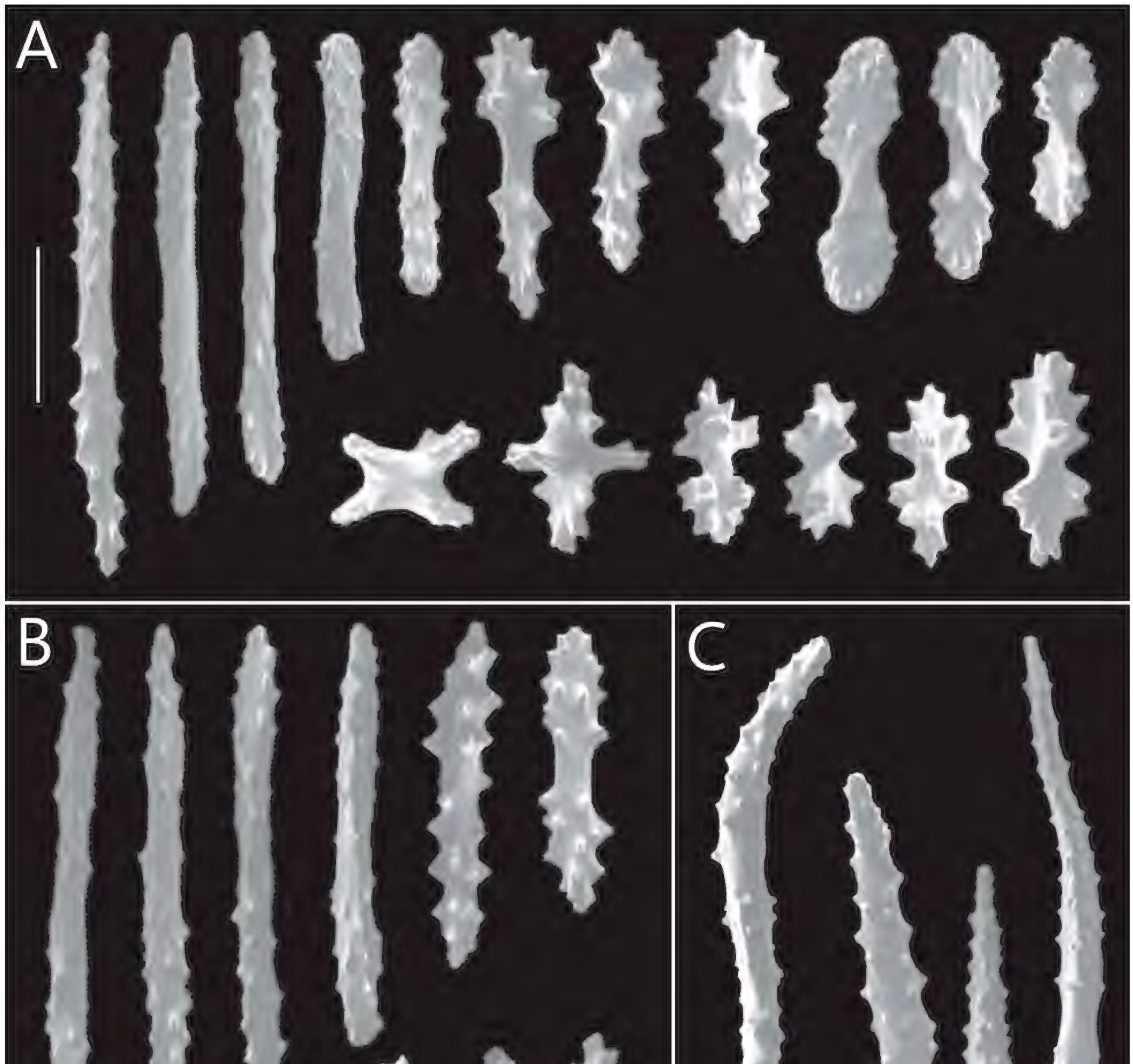

Figure 7. Sclerites of *Anthomastus mirabilis* sp. nov. (FIO-ATL83-JLBEN27711). **A.** Sclerites from anthocodial wall; **B.** Sclerites from surface of capitulum. **C.** Sclerites from interior of capitulum. Scale bars: 0.10 mm.

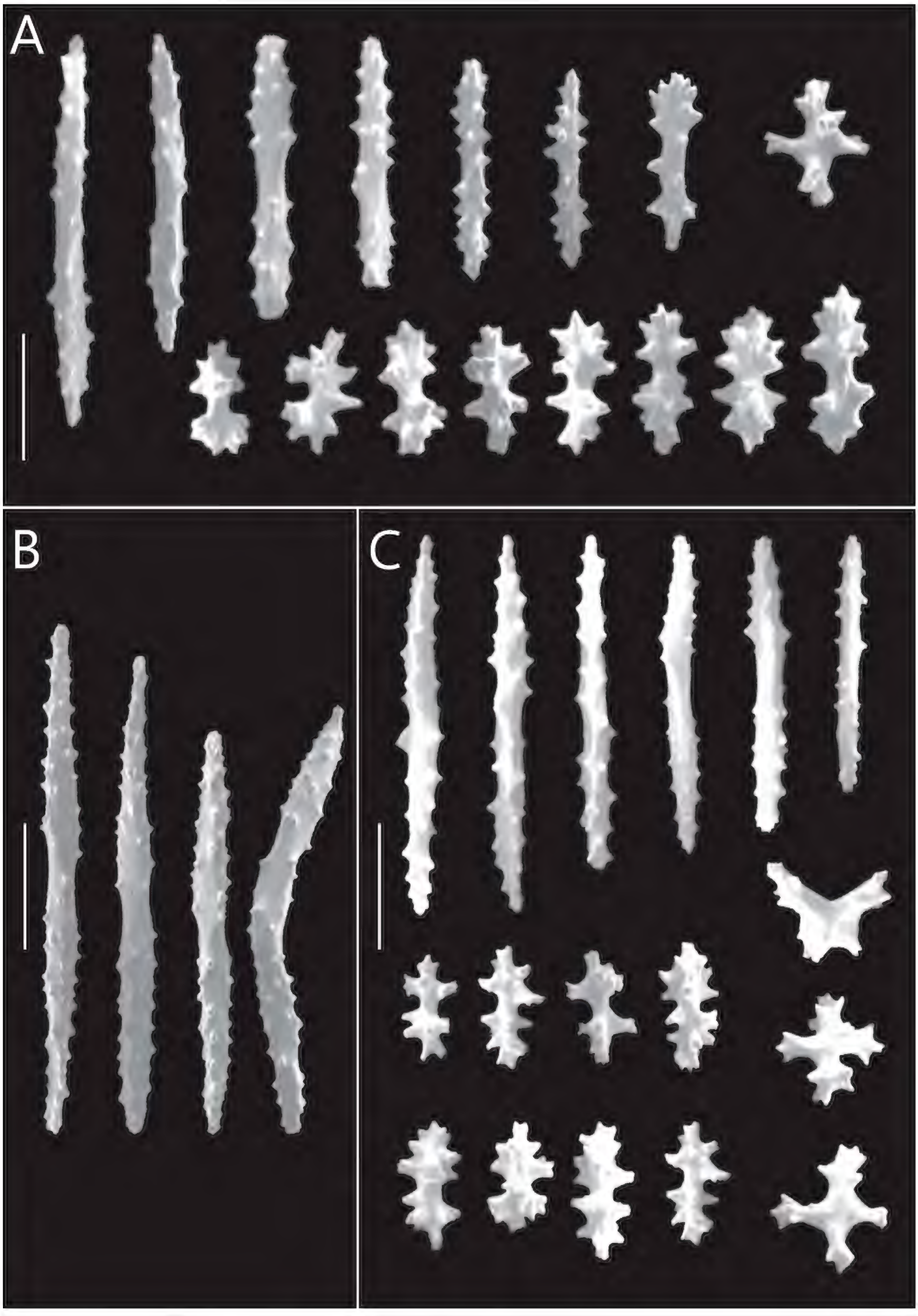

Figure 8. Sclerites of *Anthomastus mirabilis* sp. nov. (FIO-ATL83-JLBEN27711). **A.** Sclerites from surface of stalk; **B.** Sclerites from interior of stalk; **C.** Sclerites from holdfast. Scale bars: 0.10 mm.

The new species also closely resembles *A. gyratus*. While both share similar sclerite morphology, *A. mirabilis* sp. nov. is separated because its autozooids are distributed across the entire capitulum, whereas in *A. gyratus*, they are arranged only over the distal three-quarters of the capitulum; furthermore, *A. mirabilis* sp. nov. lacks spindles and has dumbbells present in the anthocodial tentacles and wall, a combination not found in *A. gyratus*. The unique traits of *A. mirabilis* sp. nov. also exclude it from all remaining *Anthomastus* species. It differs from *A. bayeri* by the presence of pharyngeal sclerites. It is separated from *A. nanhaiensis* and *A. tongi* because its tentacular sclerites are more diverse and include plates, unlike the rods-exclusive composition of the latter two. Finally, its composition of predominantly platelet-type pharyngeal sclerites and its unique sclerite combination (dumbbells present, spindles absent) clearly distinguish it from all other *Anthomastus* species that either have different pharyngeal sclerite types (e.g., *A. megacephalus*) or different overall sclerite profiles (e.g., *A. globosus* and *A. antarcticus*). The combination of having dumbbells and plates in the tentacles while lacking spindles throughout the colony provides robust and comprehensive morphological evidence to support the designation of *A. mirabilis* as a distinct new species.

Molecular phylogenetics

The mitochondrial genome of *Neoanthomastus longistylus* sp. nov. is circular, with a total length of 19,102 bp, and encodes 14 PCGs, 2 ribosomal RNA (rRNA) genes, and 1 transfer RNA (tRNA) gene (Fig. 9A). While the mitochondrial genome of *Anthomastus mirabilis* sp. nov. is also circular but longer, with a total length of 20,435 bp (Fig. 9B). It contains 17 PCGs, 2 rRNA genes, and 1 tRNA gene. The additional three PCGs result from duplications of *ND6*, *ND3*, and *ND4L*. Pairwise sequence alignment showed that the duplicated gene copies were completely identical at the nucleotide level, with no frameshift mutations, stop codon disruptions, or non-synonymous substitutions. To further confirm the presence of these duplicated genes, four pairs of specific primers were designed using Primer5 (Suppl. material 1: table S1) to target the duplicated regions of *ND6*, *ND3*, *and ND4L*. The sequencing results from three samples verified that each of the three genes occurs in two distinct loci within the mitochondrial genome (Fig. 9C).

The phylogenetic relationships within the subfamily Anthomastinae were reconstructed based on two independent datasets: the mitochondrial genome (13 PCGs) and the partial *mtMutS* gene (Figs 10, 11). Both Bayesian Inference (BI) and Maximum Likelihood (ML) analyses of each dataset yielded congruent and well-supported topologies. These phylogenetic trees consistently resolved species within Anthomastinae into five distinct clades. The phylogenetic analyses robustly support the placement of *N. longistylus* sp. nov. within the *Neoanthomastus* clade and *A. mirabilis* sp. nov. within the *Anthomastus* clade, consistent with the clades identified by (Li et al. 2025).

The interspecific genetic distance based on 14 PCGs between *Neoanthomastus longistylus* sp. nov. and *N. stellatus* was shortest at 0.0339% (Suppl. material 1: table S4). *Anthomastus mirabilis* sp. nov. and *A. grandiflorus* showed the shortest interspecific genetic distance at 0.0205% (Suppl. material 1: table S5). Additionally, the intraspecific genetic distances for both *N. longistylus* sp. nov. and *A. mirabilis* sp. nov. were zero.

Discussion and conclusions

Mushroom soft corals are the least studied among Coralliidae. This study reports the discovery of two new species, *Neoanthomastus longistylus* sp. nov. and *Anthomastus mirabilis* sp. nov., collected from the Southern Mid-Atlantic Ridge. Based on 14 PCGs, both these new species exhibited relatively small genetic distances to their closest relatives, at 0.0339% and 0.0205%, respectively. Given that anthozoan mtDNA evolves markedly slowly – ~5× slower than nuclear DNA and 50–100× slower than metazoan mtDNA in general (Chen et al. 2009, Rosales Ruiz et al. 2025) – the very small mtDNA distances we report are expected and do not argue against their status as distinct species. *N. longistylus* sp. nov. is characterized by predominantly straight rods and rods with one end curved in its tentacles. *A. mirabilis* sp. nov. is distinguished by dumbbells in its tentacles and anthocodial wall, and the absence of spindles. We explicitly acknowledge that despite the support provided by the framework of Li et al. (2025), the generic boundaries, particularly those separating *Anthomastus*, *Neoanthomastus*, and *Pseudoanthomastus*, are not yet fully resolved. Our assignment of each new species to its respective genus is based on a comprehensive consideration of the latest phylogenetic framework combined with the key morphological characteristics of the new species. Future, broader molecular sampling and phylogenetic analysis will be beneficial for clarifying the boundaries between different genera and species.

The presence of multiple copies of *ND6*, *ND3*, and *ND4L* in the mitochondrial genome of *A. mirabilis* sp. nov. is a notable feature, as gene duplications in animal mitochondrial genomes are relatively rare. To confirm the presence of the duplicated genes, we performed Sanger sequencing on specific fragments, using specific primers designed to target these regions. This method allowed us to directly verify the existence of the duplicated gene sequences (Fig. 9). The fact that each gene pair in this study is 100% identical to the corresponding functional reference gene indicates that these duplicates are not pseudogenes or degraded remnants, but rather likely retain full coding potential. In the octocoral *Calicogorgia granulosa* (Malacalcyonacea, Acanthogorgiidae), a similar phenomenon was reported where its large mitogenome (20,246 bp) resulted from the duplication of a 100% identical, large segment (913 bp) containing a novel open reading frame (Park et al. 2011). Such exact duplications may have originated from tandem duplication events or genome-level recombination

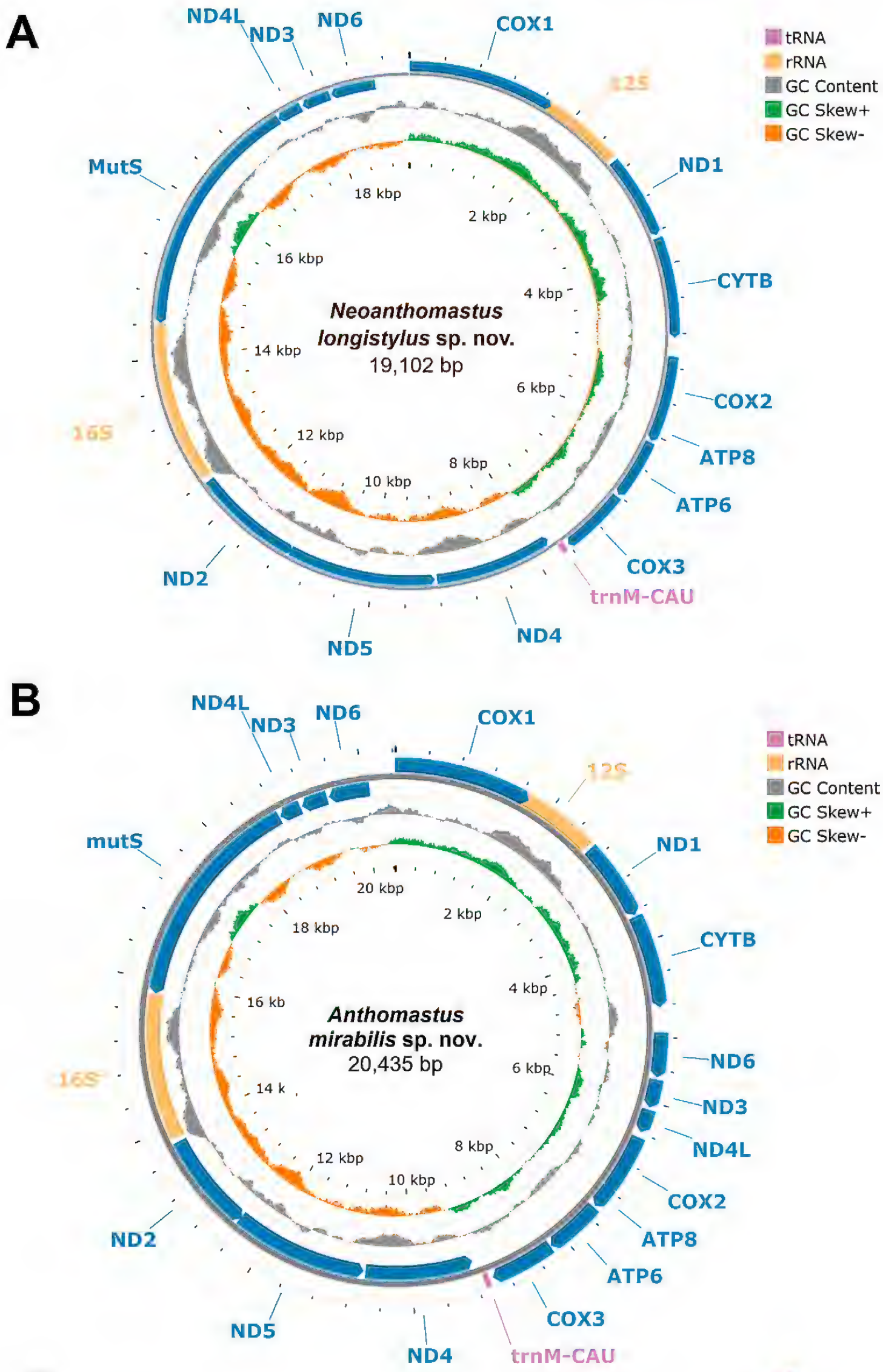

Figure 9. The complete mitochondrial genome. **A.** *Neoanthomastus longistylus* sp. nov.; **B.** *Anthomastus mirabilis* sp. nov.; **C.** Locations of PCR-amplified fragments on the mitochondrial genome of *A. mirabilis* sp. nov.

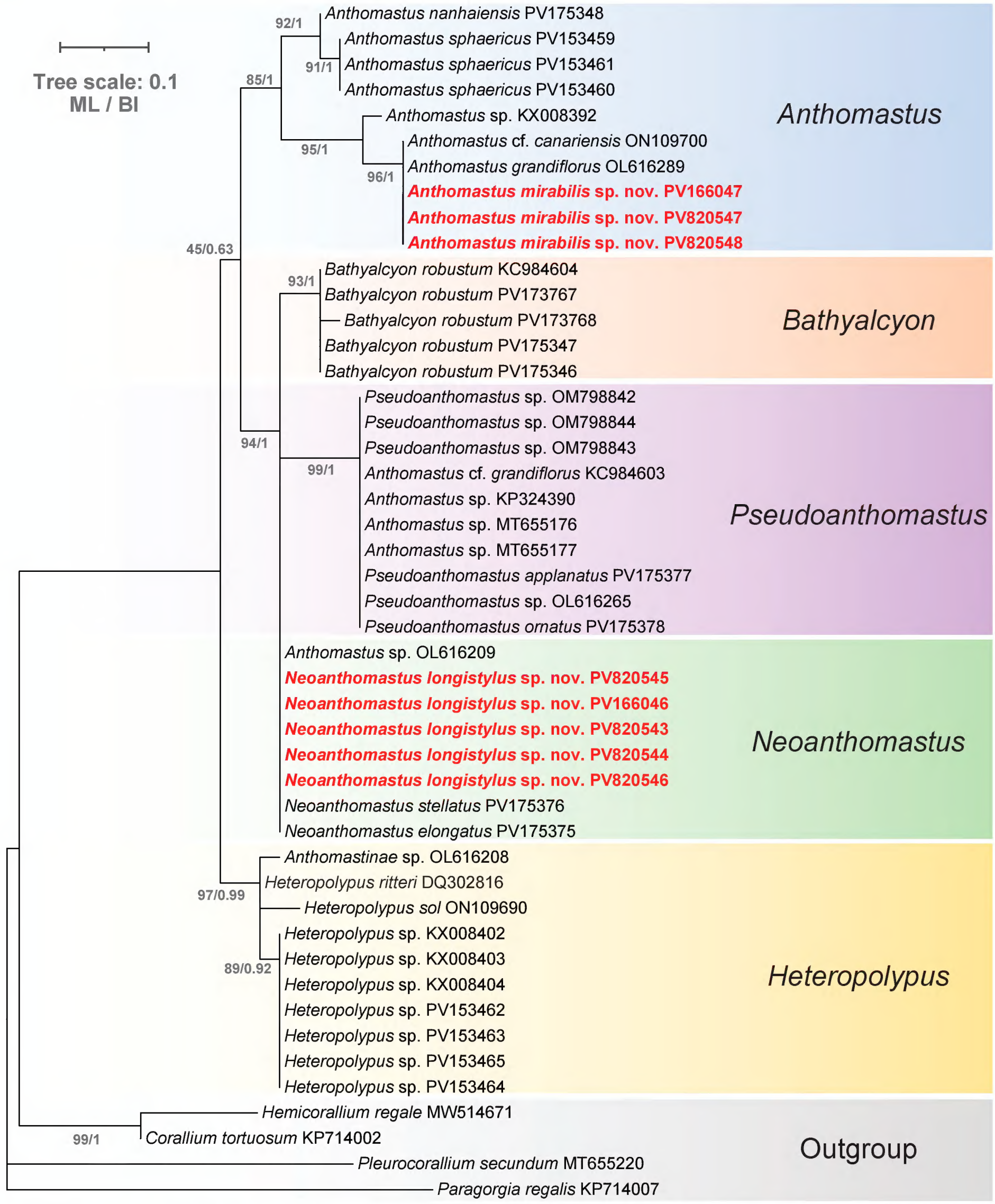

Figure 10. The phylogenetic tree of species within Anthomastinae based on the partial *mtMutS* gene. Four genera outside of Anthomastinae within Coralliidae are used as outgroups. The Maximum Likelihood (ML) tree shares the same topology as the Bayesian Inference (BI) tree, with node support values presented as: ML bootstrap values / BI posterior probabilities.

and could provide redundant or backup functions. The mitochondrial gene order of *A. mirabilis* sp. nov. and *N. longistylus* sp. nov. is identical, except for three duplicated genes of *A. mirabilis* sp. nov.. The mitochondrial genome arrangements of these two species are perfectly consistent with the *japonicum* mitochondrial gene arrangement described in Figueroa and Baco (2015, shown in their fig. 1). This *japonicum* mitochondrial gene arrangement is widely present in the family Coralliidae, serving as a characteristic gene order for the genera *Corallium* and *Hemicorallium* within this family, and differs from the *konojoi* arrangement found in the genus *Pleurocorallium*.

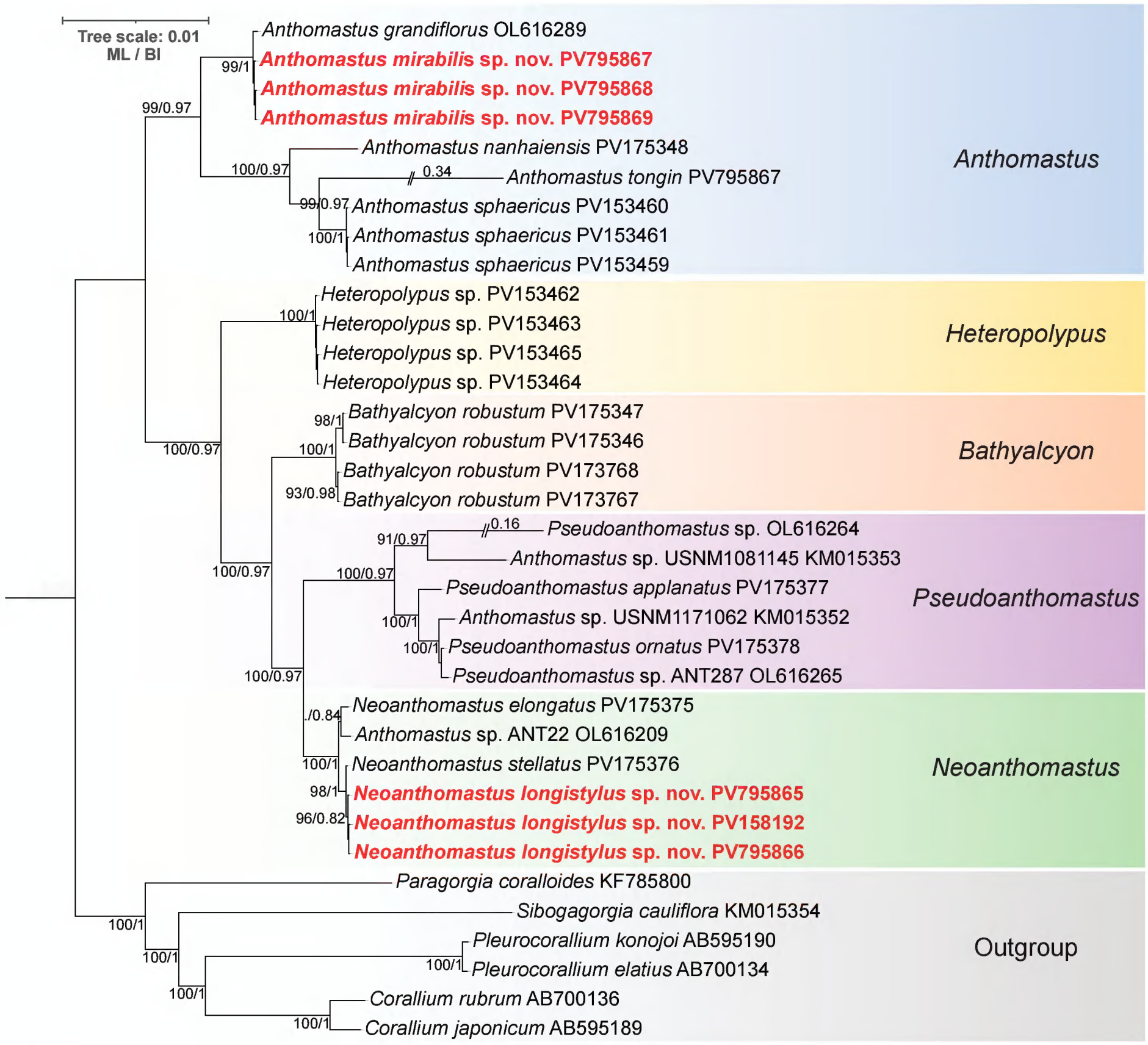

Figure 11. The phylogenetic tree of species within Anthomastinae inferred from 13 PCGs in mitochondrial genomes (*mtMutS* not included). Four genera outside of Anthomastinae within Coralliidae are used as outgroups. The Maximum Likelihood (ML) tree shares the same topology as the Bayesian Inference (BI) tree, with node support values presented as: ML bootstrap values / BI posterior probabilities.

Our phylogenetic analysis provides robust support for the division of Anthomastinae into five major clades, and the clear placement of our new species within the framework defined by Li et al. (2025) further stabilizes the subfamily's taxonomic system. However, broader taxonomic revisions remain challenging, primarily due to the scarcity of available molecular data for most Anthomastinae species. Given that this issue is compounded by potentially inaccurate annotations in public databases NCBI, we prioritized using such sequences to assess phylogenetic topology and branching patterns, rather than for definitive taxonomic validation. Future efforts should focus on filling data gaps and describing the detailed characteristics to refine the taxonomy of Anthomastinae. Taxonomic studies should integrate both molecular data and morphological characteristics to establish a more robust classification framework (McFadden et al. 2010; Hu et al. 2025).

In conclusion, this study describes two new deep-sea mushroom soft coral species, *Neoanthomastus longistylus* sp. nov. and *Anthomastus mirabilis* sp. nov., from the Southern Mid-Atlantic Ridge. The mitochondrial genomes of both species were characterized, revealing a novel duplication of three identical genes (*ND6*, *ND3*, and *ND4L*) in *A. mirabilis* sp. nov. Phylogenetic analyses using both partial *mtMutS* and 14 PCGs firmly established the evolutionary positions of these species within the subfamily Anthomastinae. Our findings significantly enrich the known biodiversity of the Southern Mid-Atlantic Ridge and provide critical baseline data for future ecological assessments and conservation efforts.

Author contributions

LXL conducted the analyses and drafted the manuscript. XQZ designed and supervised the project. XQZ and LMN collected the samples. LXL, XNX, GML and HXY performed the laboratory work. XQZ, XNX, GML, HXY, LMN, WZL, and ZXL reviewed and edited the manuscript, with all authors contributing to its revision.

Data availability statement

The data of this study are available from the corresponding author upon reasonable request.

Acknowledgements

We appreciate the invaluable support provided by the National Key R&D Program of China (No. 2023YFC2812903) and Digital Deep-sea Typical Habitats Programme of China Deep Ocean Affairs Administration. We are grateful to all scientist and crew members of *ShenhaiYihao* and the pilots of HOV *Jiaolong* during the cruise of DY83 for the sample collection, especially Yue Dong (First Institute of Oceanography, MNR), Yadong Zhou (Second Institute of Oceanography, MNR), Chengbing Song (National Deep Sea Center, MNR). We are grateful to Wenle Du (International Department, Qingdao Academy) for her experimental work and image processing efforts.

References

Bayer FM (1956) Descriptions and redescriptions of the Hawaiian octocorals collected by the US Fish Commission steamer" Albatross"(2. Gorgonacea: Scleraxonia). https://repository.si.edu/handle/10088/879

Bayer FM (1993) Two new species of the gorgonacean genus *Paragorgia* (Coelenterata: Octocorallia). http://hdl.handle.net/10088/2391

Bayer FM, Grasshoff M, Verseveldt J (1983) Illustrated trilingual glossary of morphological and anatomical terms applied to Octocorallia. Brill Archive. https://doi.org/10.1163/9789004631915

Berntson EA, Bayer FM, McArthur AG, France SC (2001) Phylogenetic relationships within the Octocorallia (Cnidaria: Anthozoa) based on nuclear 18S rRNA sequences. Marine Biology 138: 235–246. https://doi.org/10.1007/s002270000457

Carvalho NF, Waters LG, Arantes RC, Couto DM, Cavalcanti GH, Güth AZ, Falcão APC, Nagata PD, Hercos CM, Sasaki DK, Dottori M, Cordes EE, Sumida PYG (2023) Underwater surveys reveal deep-sea corals in newly explored regions of the southwest Atlantic. Communications Earth & Environment 4: 282. https://doi.org/10.1038/s43247-023-00924-0

Chen I-P, Tang C-Y, Chiou C-Y, Hsu J-H, Wei NV, Wallace CC, Muir P, Wu H, Chen CA (2009) Comparative Analyses of Coding and Noncoding DNA Regions Indicate that Acropora (Anthozoa: Scleractina) Possesses a Similar Evolutionary Tempo of Nuclear vs. Mitochondrial Genomes as in Plants. Marine Biotechnology 11: 141–152. https://doi.org/10.1007/s10126-008-9129-2

Debreuil J, Tambutté S, Zoccola D, Segonds N, Techer N, Marschal C, Allemand D, Kosuge S, Tambutté É (2011) Specific organic matrix characteristics in skeletons of *Corallium* species. Marine Biology 158: 2765–2774. https://doi.org/10.1007/s00227-011-1775-7

Figueroa DF, Baco AR (2015) Octocoral mitochondrial genomes provide insights into the phylogenetic history of gene order rearrangements, order reversals, and cnidarian phylogenetics. Genome Biology and Evolution 7: 391–409. https://doi.org/10.1093/gbe/evu286

Herrera S, Baco A, Sánchez JA (2010) Molecular systematics of the bubblegum coral genera (Paragorgiidae, Octocorallia) and description of a new deep-sea species. Molecular Phylogenetics and Evolution 55: 123–135. https://doi.org/10.1016/j.ympev.2009.12.007

Hu X, Zhang Q, Ge M, Li X, Wang Z, Zhang X, Xu Q (2025) Two new species of deep-sea Red Corals (Coralliidae, Genus *Hemicorallium* Gray, 1867) from the western Indian Ocean. Zoosystematics and Evolution 101: 317–339. https://doi.org/10.3897/zse.101.139350

Jin J-J, Yu W-B, Yang J-B, Song Y, dePamphilis CW, Yi T-S, Li D-Z (2020) GetOrganelle: A fast and versatile toolkit for accurate de novo assembly of organelle genomes. Genome Biology 21: 241. https://doi.org/10.1186/s13059-020-02154-5

Kalyaanamoorthy S, Minh BQ, Wong TK, Von Haeseler A, Jermiin LS (2017) ModelFinder: Fast model selection for accurate phylogenetic estimates. Nature Methods 14: 587–589. https://doi.org/10.1038/%20nmeth.4285

Katoh K, Standley DM (2013) MAFFT multiple sequence alignment software version 7: Improvements in performance and usability. Molecular Biology and Evolution 30: 772–780. https://doi.org/10.1093/molbev/mst010

Leão ZMAN, Kikuchi RKP (2001) The Abrolhos Reefs of Brazil. In: Seeliger U, Kjerfve B (Eds) Coastal Marine Ecosystems of Latin America. Ecological Studies. Springer, Berlin/Heidelberg, 83–96. https://doi.org/10.1007/978-3-662-04482-7_7

Li Y, Xu K (2023) *Anthomastus nanhaiensis*, new species, and Bathyalcyon robustum Versluys, 1906, two mushroom soft corals (Octocorallia: Coralliidae) from Zhenbei Seamount in the South China Sea. Raffles Bulletin of Zoology 71: 669–680. https://doi.org/10.26107/RBZ-2023-0050

Li Y, Li J, Xu K (2025) Mushroom Soft Corals (Octocorallia: Coralliidae) From Seamounts in the Tropical Northwestern Pacific: Morphology and Phylogenetic Analysis Reveal a New Genus and Six New Species. Journal of Zoological Systematics and Evolutionary Research 2025: 4177670. https://doi.org/10.1155/jzs/4177670

McFadden CS, Sánchez JA, France SC (2010) Molecular Phylogenetic Insights into the Evolution of Octocorallia: A Review. Integrative and Comparative Biology 50: 389–410. https://doi.org/10.1093/icb/icq056

McFadden CS, Van Ofwegen LP, Quattrini AM (2022) Revisionary systematics of Octocorallia (Cnidaria: Anthozoa) guided by phylogenomics. Bulletin of the Society of Systematic Biologists 1. https://doi.org/10.18061/bssb.v1i3.8735

Molodtsova TN (2013) Deep-sea mushroom soft corals (Octocorallia: Alcyonacea: Alcyoniidae) of the Northern Mid-Atlantic Ridge. Marine Biology Research 9: 488–515. https://doi.org/10.1080/17451000.2012.750427

Nguyen L-T, Schmidt HA, Von Haeseler A, Minh BQ (2015) IQ-TREE: A fast and effective stochastic algorithm for estimating maximum-likelihood phylogenies. Molecular Biology and Evolution 32: 268–274. https://doi.org/10.1093/molbev/msu300

Park E, Song J-I, Won Y-J (2011) The complete mitochondrial genome of *Calicogorgia granulosa* (Anthozoa: Octocorallia): potential gene novel-

ty in unidentified ORFs formed by repeat expansion and segmental duplication. Gene 486: 81–87. https://doi.org/10.1016/j.gene.2011.07.003

Ronquist F, Teslenko M, Van Der Mark P, Ayres DL, Darling A, Höhna S, Larget B, Liu L, Suchard MA, Huelsenbeck JP (2012) MrBayes 3.2: Efficient Bayesian phylogenetic inference and model choice across a large model space. Systematic Biology 61: 539–542. https://doi.org/10.1093/sysbio/sys029

Rosales Ruiz A, Ocaña O, De La Herrán R, Navajas-Pérez R, Ruiz Rejón C, Congil Ross A, Robles F (2025) Going deep into *Parazoanthus axinellae* (Anthozoa: Zoantharia) complex: description of two species in the Alboran Sea based on an integrative approach. Marine Biodiversity 55: 15. https://doi.org/10.1007/s12526-024-01493-x

Sánchez JA, Lasker HR, Taylor DJ (2003) Phylogenetic analyses among octocorals (Cnidaria): Mitochondrial and nuclear DNA sequences (lsu-rRNA, 16S and ssu-rRNA, 18S) support two convergent clades of branching gorgonians. Molecular Phylogenetics and Evolution 29: 31–42. https://doi.org/10.1016/S1055-7903(03)00090-3

Thomson JS (1911) The Alcyonaria of the Cape of Good Hope and Natal. Alcyonacea. Earth and Environmental Science Transactions of the Royal Society of Edinburgh 47: 549–589. https://doi.org/10.1017/S0080456800005032

Verrill AE (1879) Notice of recent additions to the marine fauna of the eastern coast of North America. American Journal of Science 3: 309–315. https://doi.org/10.2475/ajs.s3-17.100.309

Verseveldt J, Bayer FM (1988) Revision of the genera *Bellonella*, *Eleutherobia*, *Nidalia* and *Nidaliopsis* (Octocorallia: Alcyoniidae and Nidalliidae), with descriptions of two new genera. Zoölogische Verhandelingen 245: 1–131. https://repository.naturalis.nl/pub/317855

Williams GC (2003) Capitate taxa of the soft coral genus *Eleutherobia* (Octocorallia: Alcyoniidae) from Palau and South Africa; a new species and a new combination. Zoölogische Verhandelingen 345: 419–436. https://repository.naturalis.nl/pub/220576

Xiang C, Gao F, Jakovlić I, Lei H, Hu Y, Zhang H, Zou H, Wang G, Zhang D (2023) Using PhyloSuite for molecular phylogeny and tree-based analyses. iMeta 2: e87. https://doi.org/10.1002/imt2.87

Zhang D, Gao F, Jakovlić I, Zou H, Zhang J, Li WX, Wang GT (2020) PhyloSuite: An integrated and scalable desktop platform for streamlined molecular sequence data management and evolutionary phylogenetics studies. Molecular Ecology Resources 20: 348–355. https://doi.org/10.1111/1755-0998.13096

Supplementary material 1

Supplementary tables

Authors: Xinlong Li, Ningxia Xu, Meiling Ge, Xuying Hu, Mengna Li, Zongling Wang, Xuelei Zhang, Qinzeng Xu

Data type: xlsx

Explanation note: **table S1.** Primer list and PCR thermal profiles; **table S2.** The best models for Bayesian and Maximum Likelihood analysis; **table S3.** NCBI accession numbers for all samples; **table S4.** Estimates of evolutionary divergence between the species in *Neoanthomastus* measured by Kimura 2-parameter distances (%) based on 14 protein coding genes of mitochondrial genomes; **table S5.** Estimates of evolutionary divergence between the species in *Anthomastus* measured by Kimura 2-parameter distances (%) based on 14 protein coding genes of mitochondrial genomes; **table S6.** Gene fragments of *Anthomastus mirabilis* sp. nov. obtained through Sanger sequencing.

Copyright notice: This dataset is made available under the Open Database License (http://opendatacommons.org/licenses/odbl/1.0/). The Open Database License (ODbL) is a license agreement intended to allow users to freely share, modify, and use this Dataset while maintaining this same freedom for others, provided that the original source and author(s) are credited.

Link: https://doi.org/10.3897/zse.101.163559.suppl1